Parallel-chain optical transmission line for a low-loss ultraconfined light beam

Andrea Alù,[1,2,*] Pavel A. Belov,[3,4,†] and Nader Engheta[1,‡]
[1]*Department of Electrical and Systems Engineering, University of Pennsylvania, Philadelphia, Pennsylvania 19104, USA*
[2]*Department of Electrical and Computer Engineering, University of Texas at Austin, Austin, Texas 78712, USA*
[3]*Department of Electronic Engineering, Queen Mary University of London, Mile End Road, London E1 4NS, United Kingdom*
[4]*St. Petersburg State University of Information Technologies, Mechanics and Optics, Kronverksky Prospekt 49, 197101 St. Petersburg, Russia*
(Received 13 May 2009; revised manuscript received 20 July 2009; published 8 September 2009)

Linear arrays of plasmonic nanoparticles have been suggested by various groups as optical waveguides. Here, inspired by the concept of optical nanocircuits, we show that it is possible to improve the performance of such waveguide chains by pairing two of them, forming a two-wire optical transmission line. We show that choosing the operation regime near the light line may greatly reduce the effect of material absorption and disorder, still allowing field confinement in between the paired chains. Application for low-loss optical interconnects and subwavelength imaging devices are envisioned.

DOI: 10.1103/PhysRevB.80.113101 PACS number(s): 42.82.Et, 52.40.Db, 52.40.Fd, 78.66.Sq

The interface between metals and insulators is known to support optical guided modes in the form of surface plasmon polaritons, which under certain conditions may travel over several wavelengths.[1,2] If one wants to squeeze the beam so that its total transverse cross-section is subwavelength, plasmonic waveguides may be realized in the form of cylindrical waveguides (nanorods)[3,4] or linear chains of closely spaced nanoparticles.[5–17] Due to their design flexibility, the propagation properties of linear chains may be tailored at will, effectively realizing laterally confined optical connectors. Experimental realization of such devices in the nanoscale, however, has shown severe losses, mainly caused by material absorption and disorder.

At optical frequencies, both the chain and nanorod geometries are characterized by a serious trade off between field concentration and propagation losses: for beams highly concentrated around a nanoscale waveguide, which are necessarily slow wave in nature, the real part of their wave number $\mathrm{Re}[\beta]$ is usually larger than the background wave number k_0, material absorption and disorder[17] strongly affect the propagation, and the propagation distance is reduced exponentially with increase in the lateral confinement of the beam.[3,4,16] Consider, for instance, the geometries in the inset of Fig. 1(a), i.e., a chain of silver nanoparticles and a cylindrical waveguide made of silver, both of radius $a=10$ nm, embedded in a glass substrate. The period of the linear chain is $d=2.1a$, both geometries are excited with azimuthally symmetric modes with longitudinal component of electric field (analogous to the current flowing along a conducting wire at low frequencies) and in our analyses the frequency dispersion and material losses for silver, as found in the literature,[18] have been fully considered. The curves are obtained using full-wave analysis, consistent with the solutions in Refs. 4–16, which for the case of linear chains take into account all the dynamic coupling among the infinite number of particles in the array.

Figure 1 reports the propagation length (defined as the length after which the guided field is e^{-1} of the original value) and $\mathrm{Re}[\beta]/k_0$ for these two geometries, as depicted in the inset. It is evident that the cylindrical nanorod (black line) supports longer propagation length and lower attenuation constant at low frequencies (far IR), for which silver behaves as a fairly good conductor. In this regime, $\mathrm{Re}[\beta]\simeq k_0$ and, similarly to a regular thin conducting wire at microwave frequencies, the field is spread all around the cylinder in the background. If we increase the frequency of operation, up to the visible, however, $\mathrm{Re}[\beta]/k_0$ increases, together with the field confinement around the plasmonic cylindrical interface, and the propagation length is consequently reduced. The chain of nanoparticles (red lighter line) has some relevant advantages over a cylindrical nanorod: the frequency range over which $\mathrm{Re}[\beta]\simeq k_0$ may be shifted as desired up to optical frequencies by properly choosing the relevant parameters in the design. It can be seen in Fig. 1 that in this specific example the chain hits the light line ($\mathrm{Re}[\beta]=k_0$) in the mid visible ($f=560$ THz, green light), and consequently a substantial improvement in the propagation length may be achieved in this frequency range. The price to be paid also in this geometry, however, is the less confined beam, i.e., larger beam cross-section spread in the surrounding background material, associated with the condition $\mathrm{Re}[\beta]\simeq k_0$.

It is interesting to interpret these results in terms of optical nanocircuit theory:[19,20] since it has been shown that plasmonic and nonplasmonic nanoparticles behave equivalently as nanoinductors and nanocapacitors, respectively, then, due to the specific longitudinal orientation of the electric field, the chain of nanoparticles may be modeled as a series cascade of inductors and capacitors, representing the silver nanoparticles and the gaps separating them, as in the inset of Fig. 1(b). It is clear that a judicious choice of the nanoparticle geometry and spacing may produce a series resonance between such an LC pair, causing a short-circuit connection. In this regime, the chain is expected to effectively behave as an ideally conducting wire, as long as losses are negligible, implying the condition $\mathrm{Re}[\beta]=k_0$, even though no single material (here silver) is ideally conducting in this frequency regime. For the design of Fig. 1, this condition is satisfied at $f=560$ THz, for which the chain resembles a conducting wire with $\mathrm{Re}[\beta]=k_0$. As a consequence, the field is not much confined around this chain and instead it is spread in the background. It is evident that this frequency may be moved

at will by varying the geometry of the chain and the background material. Would it be possible to confine the beam, avoiding the field spreading associated with the condition $\mathrm{Re}[\beta]=k_0$, and at the same time still keep the advantage of low-attenuation propagation?

To this end, inspired by the solution available at microwaves and in regular circuits, we borrow the concept of two-wire transmission lines, i.e., paired conducting wires that may support transverse electromagnetic (TEM) waves confined in the space between them. By pairing together two chains of nanoparticles near their $\mathrm{Re}[\beta]=k_0$ condition we may heuristically envision an analogous behavior, which may support both highly confined fields (in the space between the chains) and relatively long propagation distances at visible frequencies. The coupling between two such identical chains of nanoparticles may be analyzed by considering both longitudinal and transverse (dominant in this regime of interest here) coupling induced between the two chains. For a single isolated chain,[16] for $e^{i\beta x}$ propagation, the corresponding guided wave number β satisfies the following closed-form adimensional dispersion relations:

$$L = 3\bar{d}^{-3}[f_3(\bar{\beta},\bar{d}) - i\bar{d}f_2(\bar{\beta},\bar{d})] - \bar{\alpha}^{-1} = 0,$$

$$T = -\frac{3}{2}\bar{d}^{-3}[f_3(\bar{\beta},\bar{d}) - i\bar{d}f_2(\bar{\beta},\bar{d}) - \bar{d}^2 f_1(\bar{\beta},\bar{d})] - \bar{\alpha}^{-1} = 0, \quad (1)$$

for longitudinal and transverse modes, respectively, where $f_N(\bar{\beta},\bar{d})=Li_N(e^{i(\bar{\beta}+1)\bar{d}})+Li_N(e^{-i(\bar{\beta}-1)\bar{d}})$, $Li_N(z)$ is the polylogarithm function of order N (Ref. 21) and all the quantities have been normalized, consistent with Ref. 16, as $\bar{d}=k_0 d$, $\bar{\beta}=\beta/k_0$, and $\bar{\alpha}=k_0^3\alpha/(6\pi\varepsilon_0)$. Implicitly, an $e^{-i2\pi ft}$ time convention has been assumed.

When l is finite in Fig. 1, the coupling between the two chains implies a modification of their guidance properties, which may be taken into account by considering the polarization fields induced by each chain on the other. In the limit of interest here, and for this polarization of interest, the dominant contribution from one to the other chain is provided by the first-order cylindrical mode supported by each chain. Specifically, as described in Ref. 16, at sufficient distance from the dipoles, each chain may be described as an averaged current line with amplitude $-i\omega\mathbf{p}e^{i\beta z}/d$, with $\mathbf{p}$ being the eigenvector corresponding to the solution of Eq. (1). Each current line radiates a dominant cylindrical wave with vector potential

$$\mathbf{A} = \frac{\omega\mu_0}{4}\mathbf{p}H_0^{(1)}(\sqrt{k_0^2-\beta^2}\rho)e^{i\beta z}, \quad (2)$$

where $H_n^{(1)}$ is the cylindrical Hankel function of first kind with order n and ρ is the radial coordinate in the cylindrical reference system. This radiation contributes an additional polarization field on the other chain, which may be described in terms of coupling coefficients between the two chains.

The final closed-form dispersion relation for the coupled modes, providing the modal dispersion for this geometry, may be obtained as

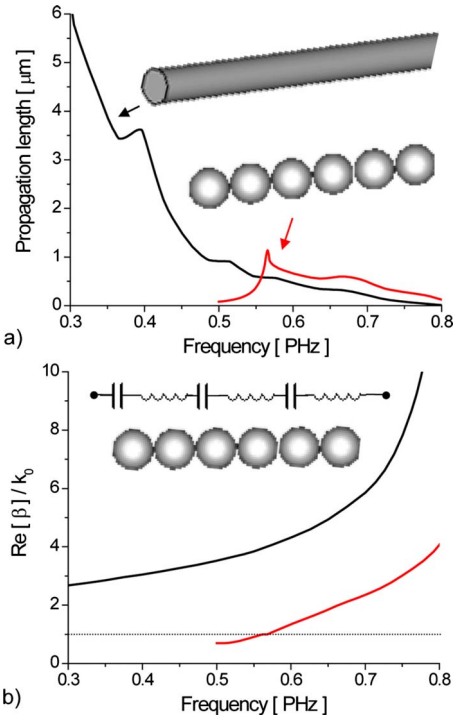

FIG. 1. (Color online) Propagation properties of linear plasmonic waveguides. (a) Frequency dispersion of propagation length and (b) guided wave number for a cylindrical nanorod made of silver and for a linear chain of spherical silver nanoparticles, as in the inset of panel (a). Both geometries have radius $a=10$ nm, the chain period is $d=2.1a$. In the inset of panel (b): nanocircuit model of a chain of plasmonic nanoparticles. At the crossing of the wave number with the light line, the nanoinductors and nanocapacitors support a series resonance, with guidance properties analogous to those of an ideally conducting wire at low frequencies.

$$\det\begin{pmatrix} L & 0 & C_{LL} & C_{LT} \\ 0 & T & C_{LT} & C_{TT} \\ C_{LL} & -C_{LT} & L & 0 \\ -C_{LT} & C_{TT} & 0 & T \end{pmatrix} = 0, \quad (3)$$

where L and T are given in Eq. (1) and the coupling terms C are given below by the corresponding Hankel functions for the electric field induced on the parallel chains using Eq. (2)

$$C_{LL} = i\frac{3\pi}{2\bar{d}}(1-\bar{\beta}^2)H_0^{(1)}[\sqrt{1-\bar{\beta}^2}\bar{l}],$$

$$C_{LT} = \frac{3\pi}{2\bar{d}}\bar{\beta}\sqrt{1-\bar{\beta}^2}H_1^{(1)}[\sqrt{1-\bar{\beta}^2}\bar{l}],$$

$$C_{TT} = i\frac{3\pi}{2\bar{l}\bar{d}}\{\sqrt{1-\bar{\beta}^2}H_1^{(1)}[\sqrt{1-\bar{\beta}^2}\bar{l}] + \bar{\beta}^2\bar{l}H_0^{(1)}[\sqrt{1-\bar{\beta}^2}\bar{l}]\}. \quad (4)$$

Equations (3) and (4) ensure a closed-form solution for the normalized complex wave number $\bar{\beta}$ of the modes supported by such twin chains of nanoparticles, as a function of their normalized period $\bar{d}$ and normalized distance between them $\bar{l}=k_0 l$. These coefficients are valid as long as $\bar{l}>2\bar{d}$, i.e., the coupling is not too strong. More rigorous coupling coefficients may be derived in terms of summations of Floquet

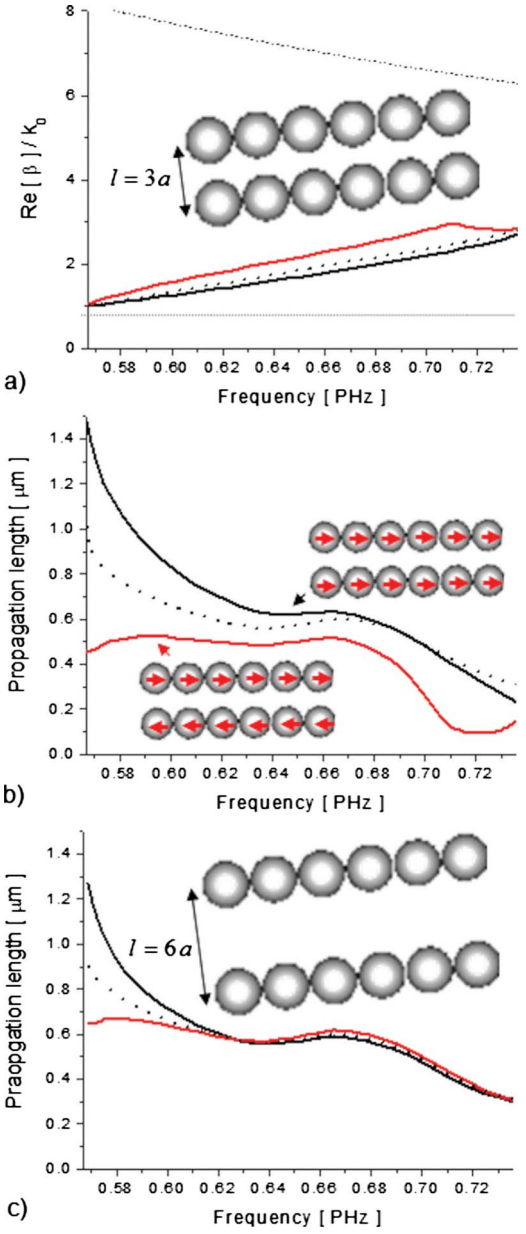

FIG. 2. (Color online) Optical two-wire nanotransmission lines. (a) Dispersion of the guided wave number and (b) propagation length for two parallel chains as in Fig. 1, with separation $l=3a$, comparing the antisymmetric (red lighter line) and symmetric (black solid) modes, together with the isolated chain (black dotted). The thin lines on the top and bottom of panel (a) indicate the first Bragg resonance and the light line, respectively. Panel (c) shows the propagation length for $l=6a$ (due to much reduced coupling, the wave number in this case is very similar in coupled and uncoupled geometries and it has not been reported).

modes from the chains for tighter coupling, but this is beyond the interest of the present Brief Report.

The coupled modes supported by this geometry, as depicted in the inset of Fig. 2(b), induce two distinct longitudinal modes, one with symmetric distribution of the polarization currents along two chains (black lines), the other with antisymmetric properties (red lines). Clearly, we are interested in this latter mode, which resembles the current in the

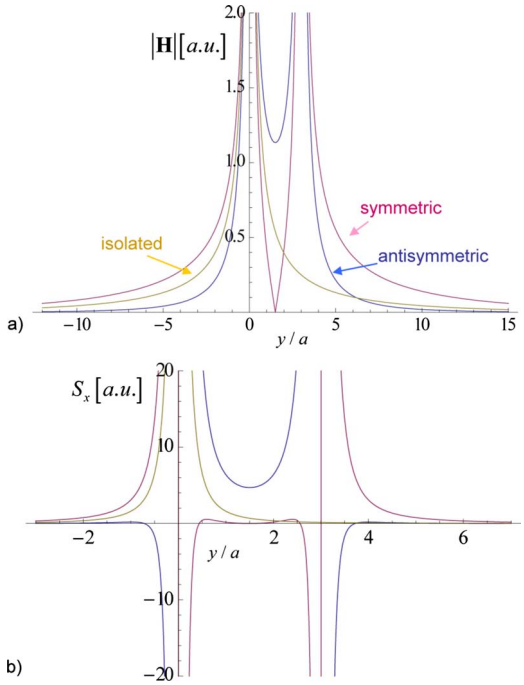

FIG. 3. (Color online) (a) Amplitude of the magnetic field and (b) power flux density distribution on a transverse cut across the line connecting the two chains for the geometry of Figs. 2(a) and 2(b), comparing the three different modes under analysis. For simplicity of model, the chains have been represented in these field plots with their averaged current density along their axis, which model well the field distribution in the background region. The strong field and power flow confinement provided by the antisymmetric (nanotransmission-line) operation is evident here.

two-wire transmission lines. Figure 2 reports the variation in $\mathrm{Re}[\beta]/k_0$ and the propagation distance for these two modes, compared with those of an isolated chain. In this example, the distance between the chains is $l=3a$ for Figs. 2(a) and 2(b) and $l=6a$ for Fig. 2(c).

It can be seen from Fig. 2 that the propagation distance for the twin chains is only slightly deteriorated for the antisymmetric mode, when compared to the isolated chain, but at the advantage of a much more confined beam traveling in the space between the two chains, due to the oppositely directed (i.e., antisymmetric) polarization currents traveling along the chains. Working exactly at the light line is not convenient due to the strong unwanted transverse coupling. However, at slightly higher frequencies and over a relatively wide frequency range spanning green and blue lights in this example, the antisymmetric mode may still operate relatively close to the light line, ensuring both low attenuation and high field confinement between the two chains. Increasing the distance between the chains, as in Fig. 2(c), may further improve the situation, allowing optimum field guidance over several wavelengths.

Figure 3 reports the distributions of the transverse (normal to the plane of the figure) magnetic field and real part of the Poynting vector (power flow) on the y axis (cross-sectional line connecting the two chains) for the geometry of Figs. 2(a) and 2(b) at the frequency $f=585$ THz. The antisymmetric and symmetric modes, together with the case of an isolated

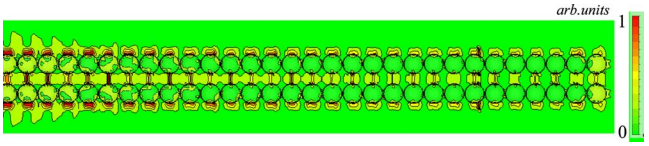

FIG. 4. (Color online) Full-wave simulations of the magnitude of the transverse electric field along a finite twin chains, two wavelengths long, as evaluated with commercial software, Ref. 22, for the geometry of Figs. 2(a) and 2(b), considering antisymmetric (nanotransmission-line) excitation.

chain, are shown. It is evident that the antisymmetric mode provides huge field and power flow confinement in the region between the chains, not only better than the symmetric scenario but also even better than the isolated chain. This is analogous to the operation of a two-wire transmission line at radio frequencies, and it is independent of the chain separation l. We have confirmed these results with full-wave numerical simulations, obtained with commercial software based on a finite-integration technique,[22] fully taking into account the nanoparticle geometry and the finite length of the chain, together with realistic losses and frequency dispersion of silver from an appropriate Drude model.[18] In Fig. 4 we have reported, as an example, the amplitude of the transverse electric field distribution in the geometry of Figs. 2(a) and 2(b) at frequency $f=585$ THz, as extracted from the simulations using the commercial software.[22] We have verified that these simulations fully confirm the full-wave analytical results reported above, both from a qualitative and a quantitative point of view. In addition, Ref. 23 reports a time-domain animation for this geometry, underlining the guidance of optical beam in these optical two-wire nanotransmission lines. It is noticed that longer propagation lengths may be achieved with larger nanoparticles, consistent with our results for individual linear arrays.[16] In this case, also higher level of material losses may become more manageable, for instance, allowing us to employ gold or other plasmonic materials, arguably having some advantages from the technological standpoint, but usually higher absorption than silver. The above analysis may fully take into account the effects of material losses and size variation, analogous to what was presented in Ref. 16. We will present a complete analysis applied to this parallel-chain configuration in a future extensive paper.

There may be several advantages in operating these optical nanowaveguides for different applications. The relatively long propagation distance over multiple wavelengths and strong field confinement in the (lossless) region between the two chains may be exploited for optical interconnects in nanocircuit applications, in order to connect different nanoloads at will, operating analogously to ideal connectors in low-frequency circuits. This operation has been heuristically suggested in Refs. 2, 19, and 24 and it has been fully established here with this parallel-chain geometry. Optical nanofilters analogous to those introduced in Ref. 25 and feeding lines for optical nanoantennas may be introduced following these designs.[26,27] Moreover, the tight guidance and confinement of these nanotransmission lines and their operation as quasi-TEM waveguides are ideal requisites for subwavelength imaging devices based on canalization, as those recently introduced at microwave frequencies using conducting wires in Ref. 28.

This work is supported in part by the U.S. Air Force Office of Scientific Research (AFOSR) under Grant No. FA9550-08-1-0220. P.A.B. acknowledges financial support by EPSRC through Advanced Research Fellowship under Grant No. EP/E053025/1.

*alu@mail.utexas.edu
†pavel.belov@elec.qmul.ac.uk
‡Corresponding author. engheta@ee.upenn.edu

[1] G. D. Mahan, Phys. Rev. **183**, 834 (1969).
[2] A. Alù and N. Engheta, J. Opt. Soc. Am. B **23**, 571 (2006).
[3] J. Takahara, S. Yamagishi, H. Taki, A. Morimoto, and T. Kobayashi, Opt. Lett. **22**, 475 (1997).
[4] A. Alù and N. Engheta, Radio Sci. **42**, RS6S17 (2007).
[5] M. Quinten, A. Leitner, J. R. Krenn, and F. R. Aussenegg, Opt. Lett. **23**, 1331 (1998).
[6] S. A. Tretyakov and A. J. Viitanen, Electr. Eng. **82**, 353 (2000).
[7] M. L. Brongersma, J. W. Hartman, and H. A. Atwater, Phys. Rev. B **62**, R16356 (2000).
[8] S. A. Maier, M. L. Brongersma, and H. A. Atwater, Appl. Phys. Lett. **78**, 16 (2001).
[9] S. A. Maier, P. G. Kik, and H. A. Atwater, Appl. Phys. Lett. **81**, 1714 (2002).
[10] S. A. Maier, P. G. Kik, and H. A. Atwater, Phys. Rev. B **67**, 205402 (2003).
[11] S. A. Maier, P. G. Kik, H. A. Atwater, S. Meltzer, E. Harel, B. E. Koel, and A. A. G. Requicha, Nature Mater. **2**, 229 (2003).
[12] S. K. Gray and T. Kupka, Phys. Rev. B **68**, 045415 (2003).
[13] R. A. Shore and A. D. Yaghjian, Electron. Lett. **41**, 578 (2005).
[14] R. A. Shore and A. D. Yaghjian, IEICE Trans. Commun. **E88-B**, 2346 (2005).
[15] A. J. Viitanen and S. A. Tretyakov, J. Opt. A, Pure Appl. Opt. **7**, S133 (2005).
[16] A. Alù and N. Engheta, Phys. Rev. B **74**, 205436 (2006).
[17] A. Alù and N. Engheta, in *Proceedings of the IEEE Antennas and Propagation Society (AP-S) International Symposium, Honolulu, Hawaii, 2007* (IEEE, 2007), pp. 2897–2900.
[18] P. B. Johnson and R. W. Christy, Phys. Rev. B **6**, 4370 (1972).
[19] N. Engheta, A. Salandrino, and A. Alù, Phys. Rev. Lett. **95**, 095504 (2005).
[20] N. Engheta, Science **317**, 1698 (2007).
[21] L. Lewin, *Polylogarithms and Associated Functions* (Elsevier, North-Holland, 1981).
[22] CST Studio Suite, 2008, www.cst.com
[23] See EPAPS Document No. E-PRBMDO-80-077931 for animation: transverse electric field time-domain animation for the geometry of Figs. 2(a) and 2(b), consistent with Fig. 4. The parameters of the chains are $a=10$ nm, $d=2.1a$, and $l=3a$. For more information on EPAPS, see http://www.aip.org/pubservs/epaps.html
[24] A. Alù and N. Engheta, Opt. Express **15**, 13773 (2007).
[25] A. Alù, M. Young, and N. Engheta, Phys. Rev. B **77**, 144107 (2008).
[26] A. Alù and N. Engheta, Nat. Photonics **2**, 307 (2008).
[27] A. Alù and N. Engheta, Phys. Rev. Lett. **101**, 043901 (2008).
[28] P. A. Belov, C. R. Simovski, and P. Ikonen, Phys. Rev. B **71**, 193105 (2005).